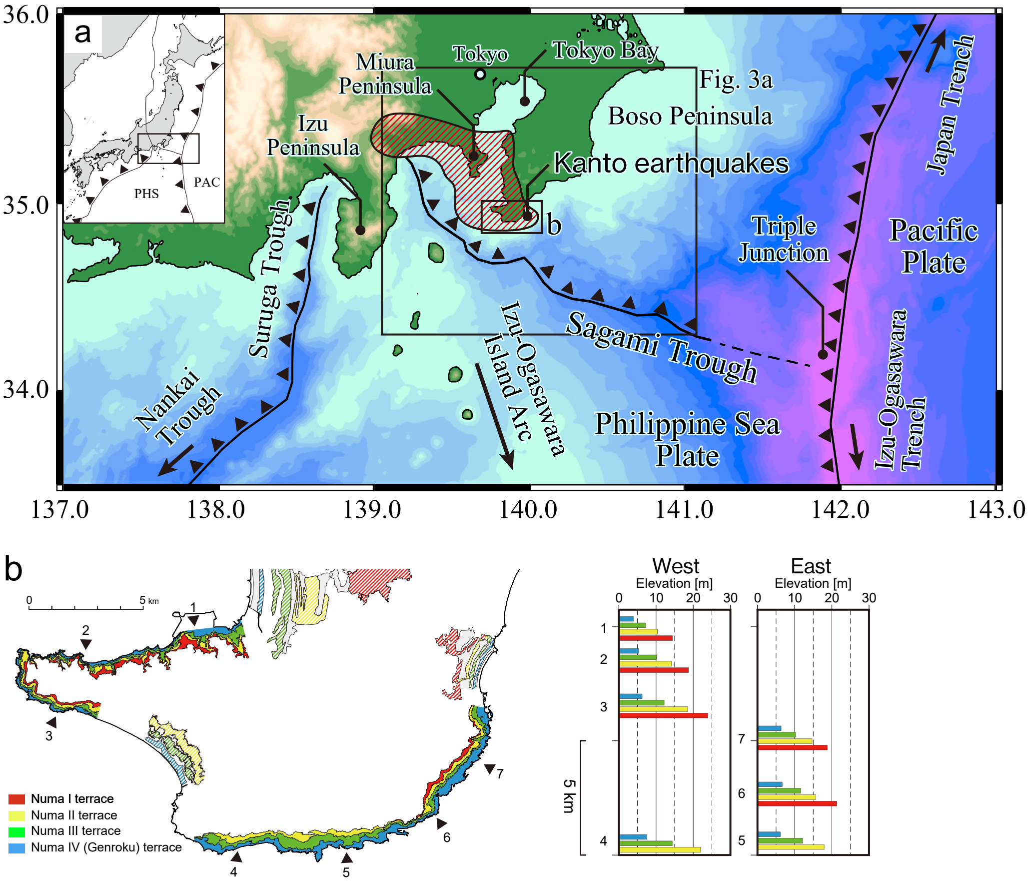

Figure 1. Survey region of this study and geological observations. (a) Tectonic setting of the Sagami Trough. The red meshed area indicates the estimated source region of the historical Kanto earthquakes (Sato et al., 2005; Sato et al., 2016). (b) Distribution of the Numa terraces after Komori et al. (2020). Right panels show the elevation distribution of the Numa terraces at each reference point, indicated by triangles in the left map.

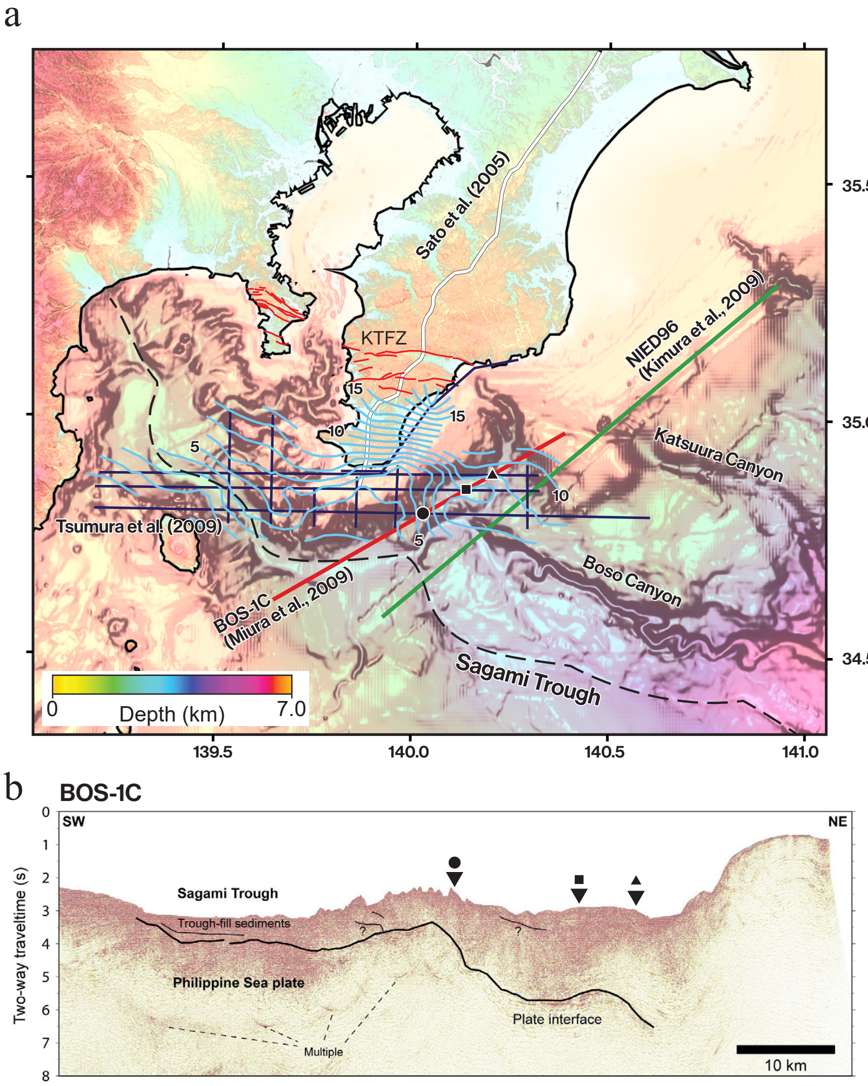

Figure 2. (a) Bathymetry map around the survey region and the profile lines of the previous reflection surveys (Sato et al., 2005; Kimura et al., 2009; Miura et al., 2009; Tsumura et al., 2009). The blue contour lines indicate the estimated depth of upper PHS by Tsumura et al. (2009), where the dark-blue straight lines are the survey profiles. The red lines indicate the inland active faults, where KTFZ stands for Kamogawa-teichi fault zone. (b) Post stack time migrated reflection image of the BOS-1C profile (Miura et al., 2009). Solid black line is our interpretation of the plate interface. Triangles indicate the positions of intersection with the survey lines of Tsumura et al. (2009).

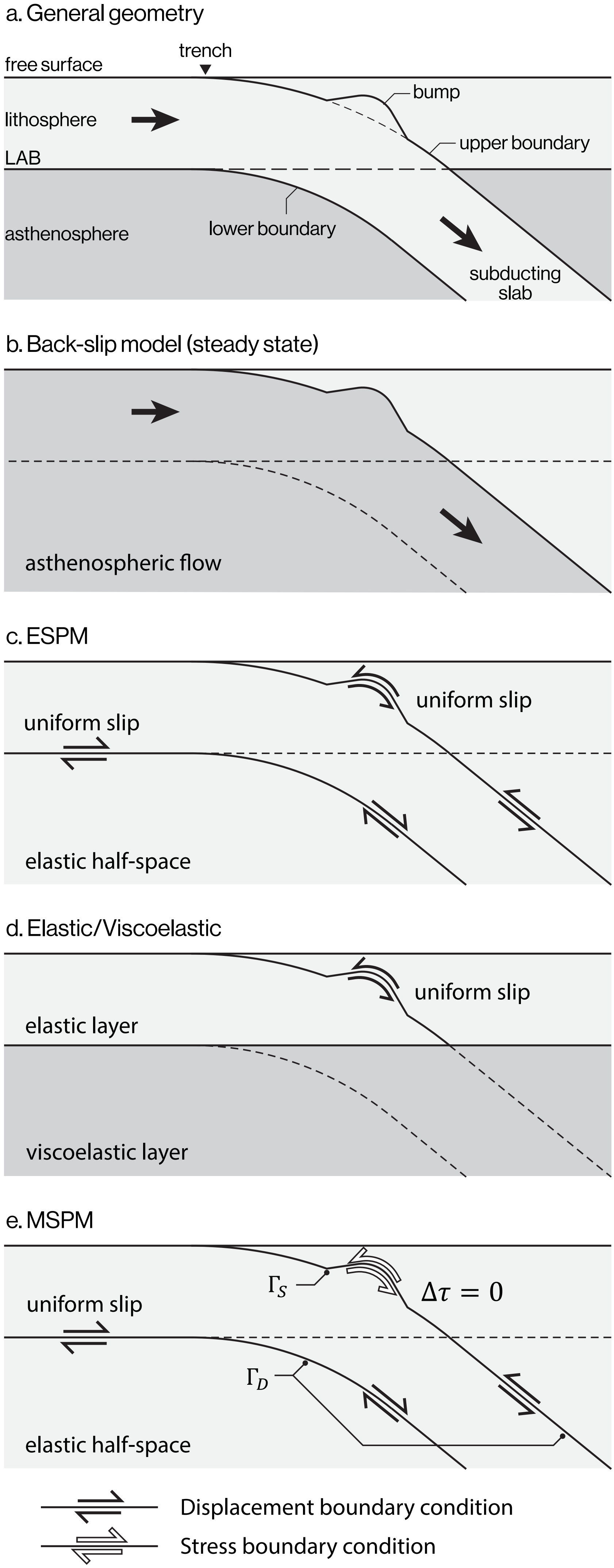

Figure 3. Schematic illustration of subduction models. (a) General geometrical setting of plate subduction. (b) Schematic representation of the imposed steady state assessed from the back-slip model, following the interpretation by Kanda and Simons (2010). (c) Slip configuration for the steady state of ESPM (Kanda and Simons, 2010). Uniform slip is imposed on the entire plate interfaces (double arrows). (d) Schematic structure illustration of the elastic/viscoelastic model. Uniform slip is imposed on the plate interface above the LAB. (e) Boundary conditions of MSPM. Black solid arrows and white arrows indicate the interfaces where uniform slip is imposed (Γ_D: area of displacement boundary condition) and no shear stress change occurs (Γ_S:area of stress boundary condition), respectively.

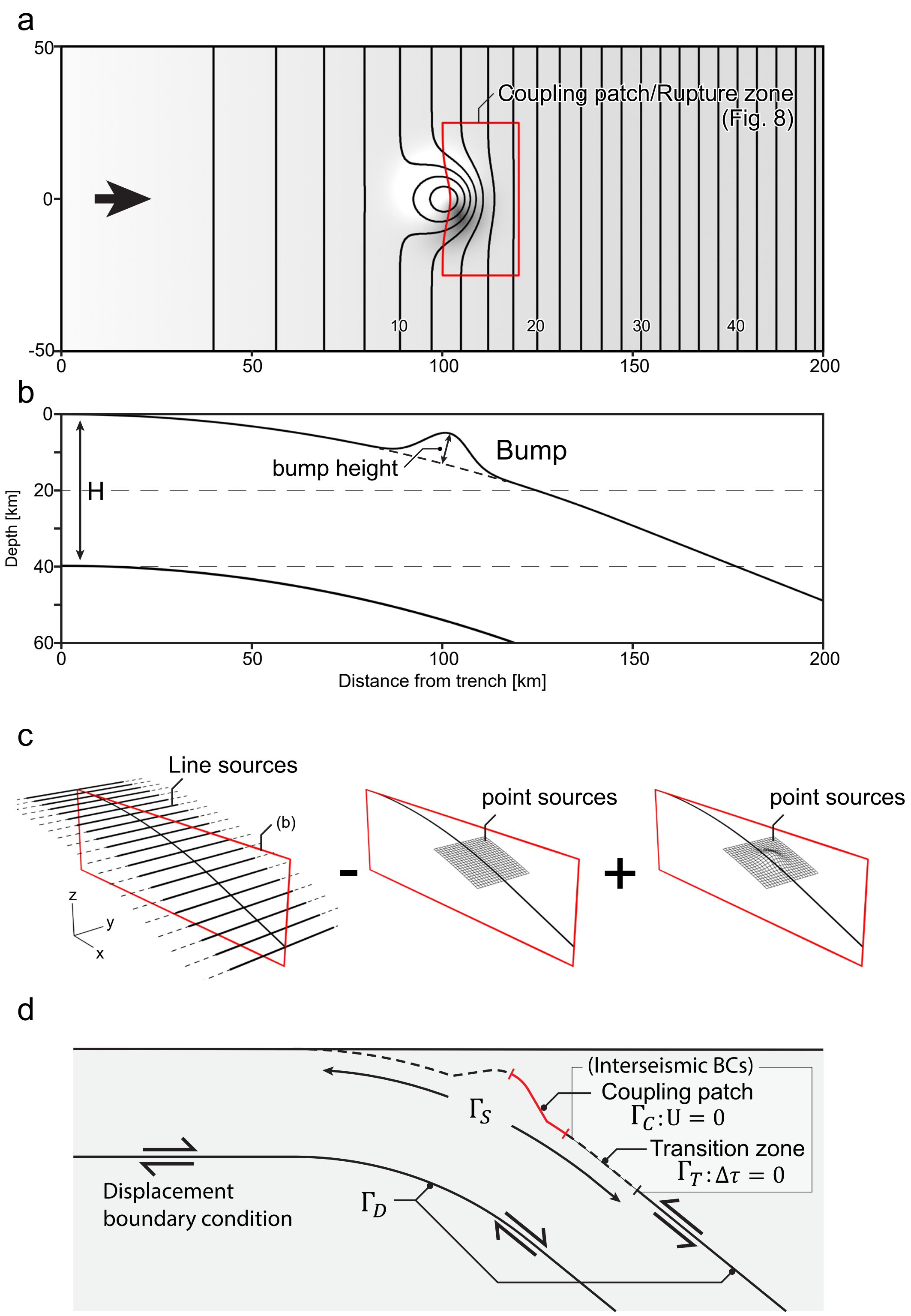

Figure 4. Geometry setting of the simple plate subduction model. (a) Plan view of the upper plate interface. The black lines indicate depth contours at 2 km interval. A conical-shaped bump with a height of 8 km is positioned at a depth of 10 km. The red rectangle indicates the rupture area and coupling patch in the earthquake sequence examination (Figure 8) (b) Cross-sectional view of the model geometry. The lower plate interface is set with a thickness H for ESPM and MSPM. (c) Schematic illustration of the superposition calculation used in the elastic/viscoelastic model. Refer to the main text for an explanation of this assumption. (d) Division of plate interfaces and boundary conditions in the earthquake sequence model using MSPM. The red and black broken lines correspond to the coupling patch and transition zone, respectively, applied during the interseismic period. The stress boundary condition is applied to the entire Γ_S during steady-state and coseismic events. The displacement boundary condition is applied to Γ_D during steady-state and the interseismic period.

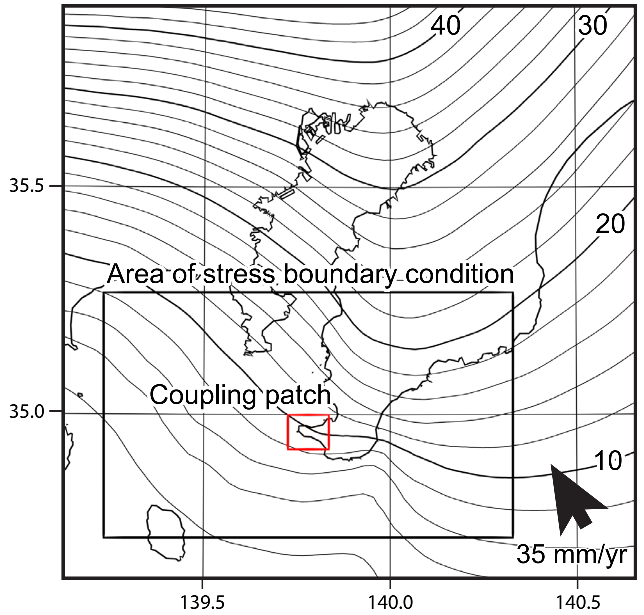

Figure 5. Geometry setting of the model simulation for the Sagami Trough subduction zone. The contour is the depth distribution of the upper plate interface of PHS, referring to Hashimoto et al. (2004), Hirose et al. (2008), and Tsumura et al. (2009). The black rectangle indicates the AOS, including a coupling patch for the earthquake sequence model, denoted by the red rectangle. Outside of the AOS is steady slip area, where uniform slip is imposed in the direction indicated by the arrow.

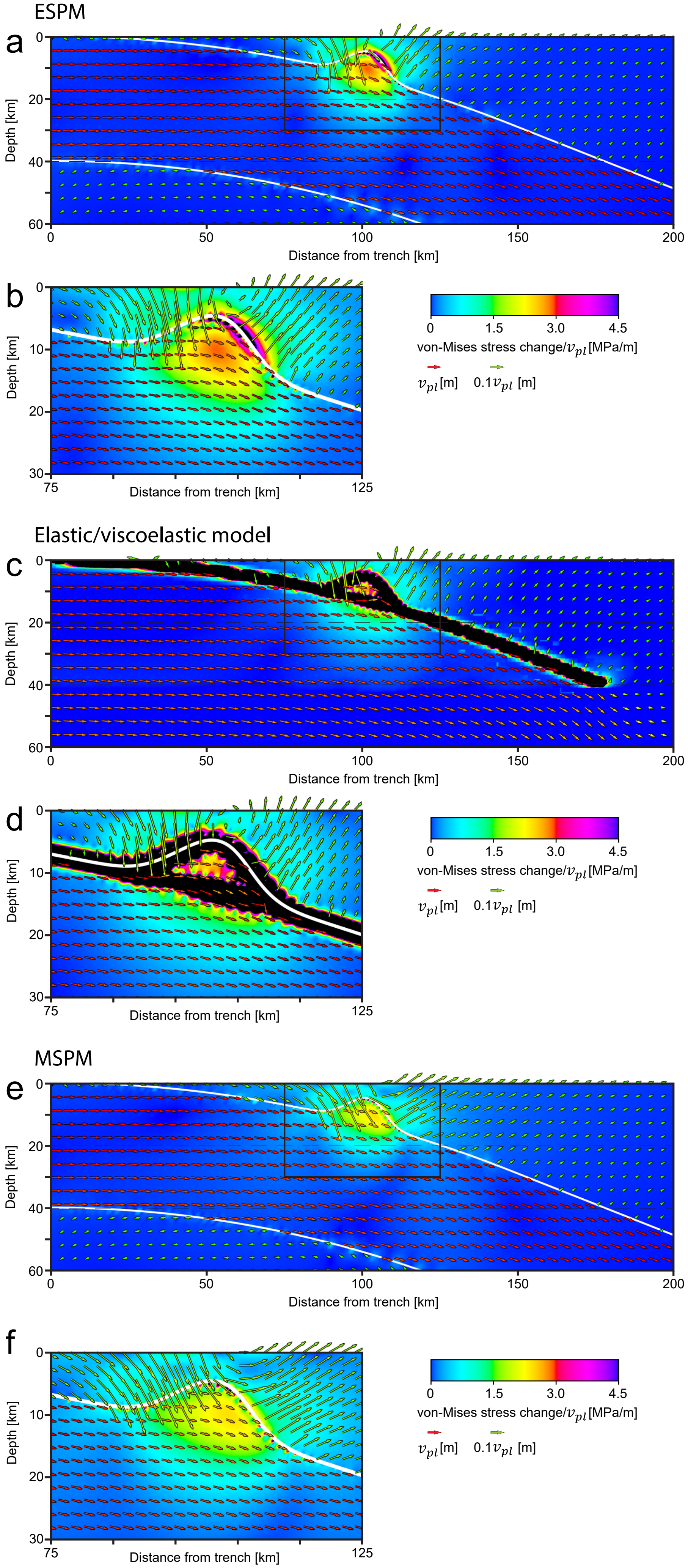

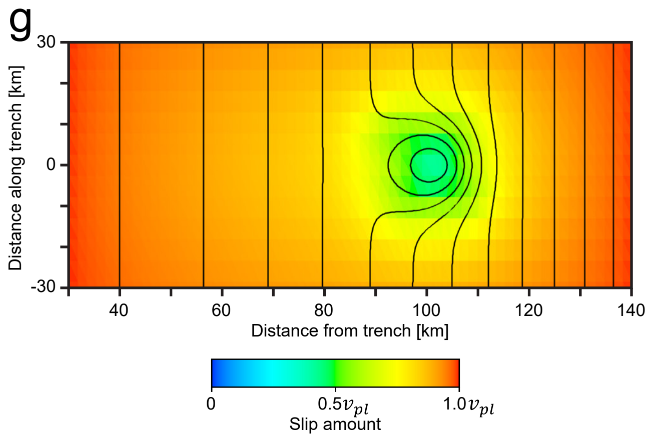

Figure 6. Simulation results of the subduction models with the simple plate geometry. (a and b) Results of ESPM. (c and d) Results of the elastic/viscoelastic model. (e and f) Results of MSPM. (a, c, and e) Displacements (arrows) and stress change distribution (color map) showing the overall cross-sectional view. Black color represents greater than 4.5 MPa/m, namely singular value. The white solid lines and dashed lines depict the plate interfaces and the depth of LAB, respectively. The arrows outside the slab (bluish colored) are exaggerated by ten times than those inside the slab. (b, d, and f) Close-up view around the bump geometry. The extension is shown by the rectangle in the overall view. (g) Slip rate distribution on the plate interface using MSPM, relative to unit slip rate V. Contour lines indicate the depth of the plate interface by 2 km interval, same as Figure 4a.

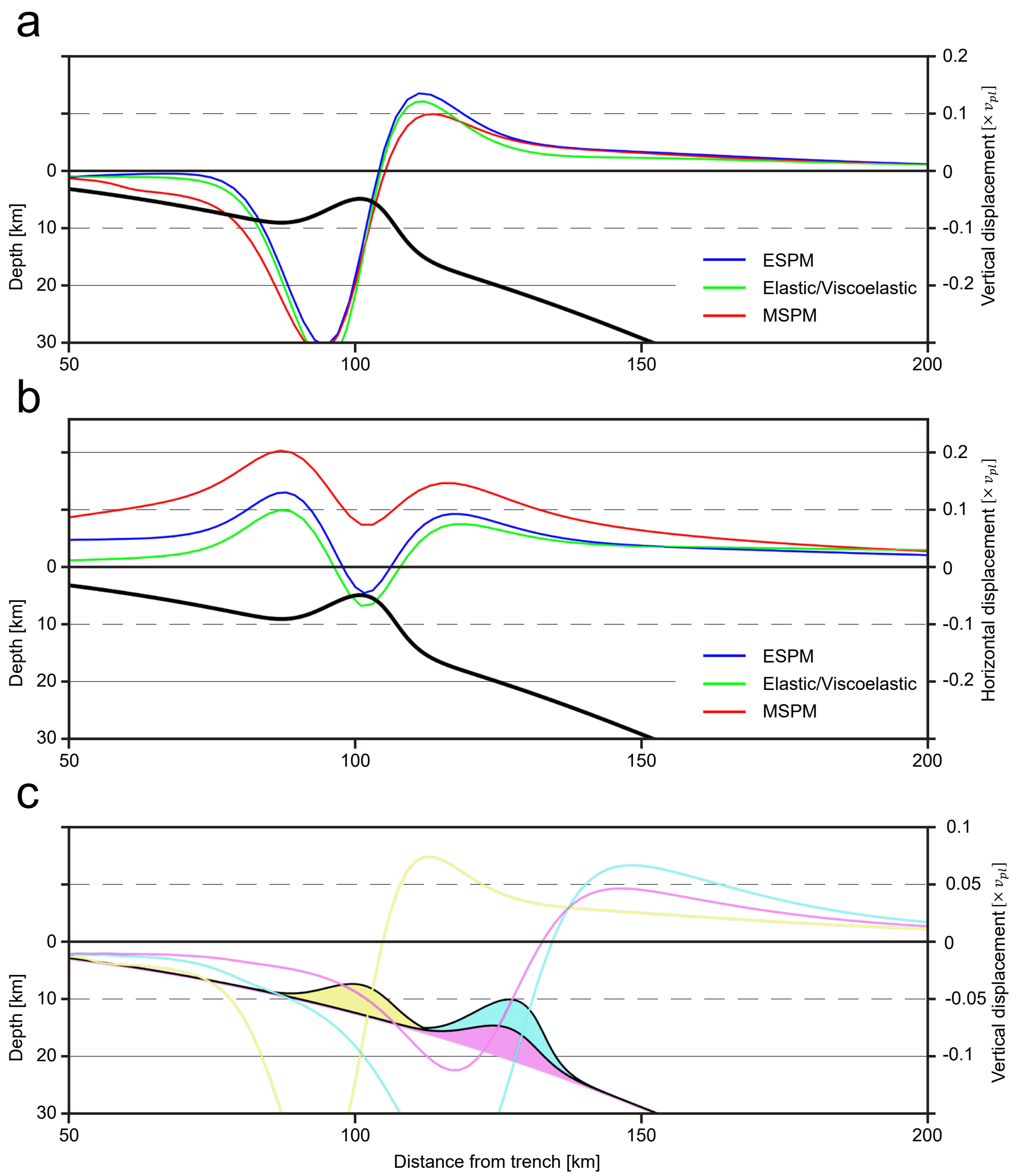

Figure 7. (a and b) Vertical and horizontal displacement distribution in each model. These results correspond to the arrows on the surface depicted in Figures 6 a, c, and e. Positive value indicates movements towards the subduction direction in (b). (c) Vertical displacement distributions with different bump geometries. The line colours correspond to the geometries of subducted seamounts. MSPM model was used for these simulations.

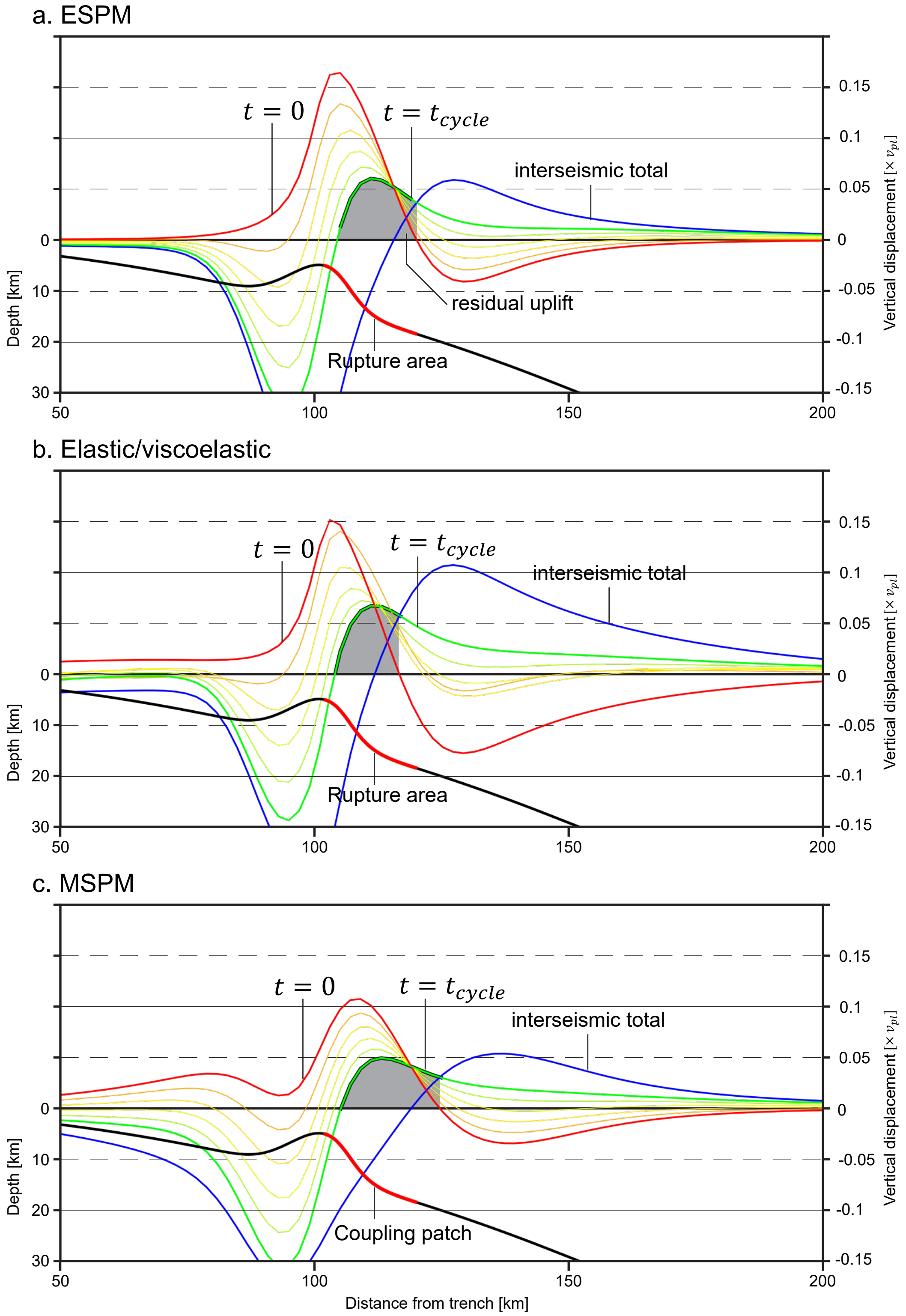

Figure 8. Transition of vertical displacements resulting from the earthquake sequence models. The red portion of the plate interface geometry indicates range pf the rupture area (ESPM and Elastic/viscoelastic model) and coupling patch (MSPM), as shown in Figure 4. Red lines present the coseismic vertical deformation at t=0 and transits into the terminal deformation pattern at t=t_cycle depicted by the green lines. Yellow lines represent the snapshots of this transition at every 1/5 t_cycle. The differences between red and green lines are interseismic total deformation, which is depicted by the blue lines. The shaded portions of the green lines indicate the residual uplift, where uplifts are observed both in coseismic and terminal deformation patterns.

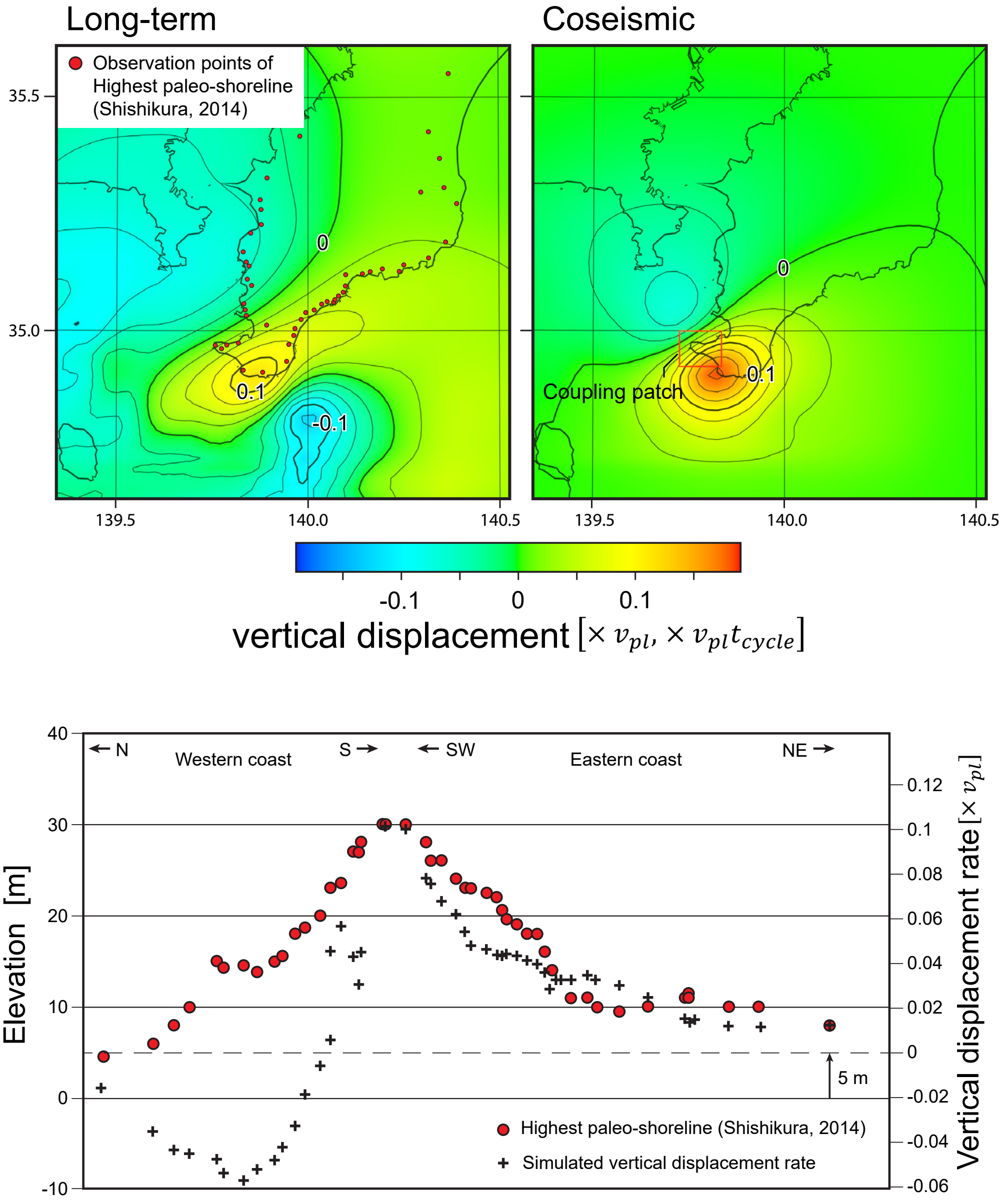

Figure 9. Simulated deformation distributions using MSPM with the model geometry of the Sagami Trough subduction zone. (a) Vertical displacement rate distribution with the steady-state assumption. (b) Coseismic vertical deformation distribution with the coupling patch representing the 1703 event, depicted by the red rectangle. (c) Comparison between the observed elevation distribution of the highest Holocene paleo-shoreline (Shishikura, 2014) and simulated vertical displacement rate. Observation points are displayed in (a). The amplitude of vertical displacement is calibrated assuming that the convergence rate and the age of the highest Holocene sea level are 35 mm/year and 7,000 BP. The vertical displacement is shifted by 5 meters reflecting the Holocene highstand.